16/04/2024

Laura Rodríguez García
ESA Research Fellow

Acceleration and Transport of Solar Energetic Particles in the Inner Heliosphere

How do solar eruptions produce energetic particle radiation that fills the heliosphere?

Particle acceleration

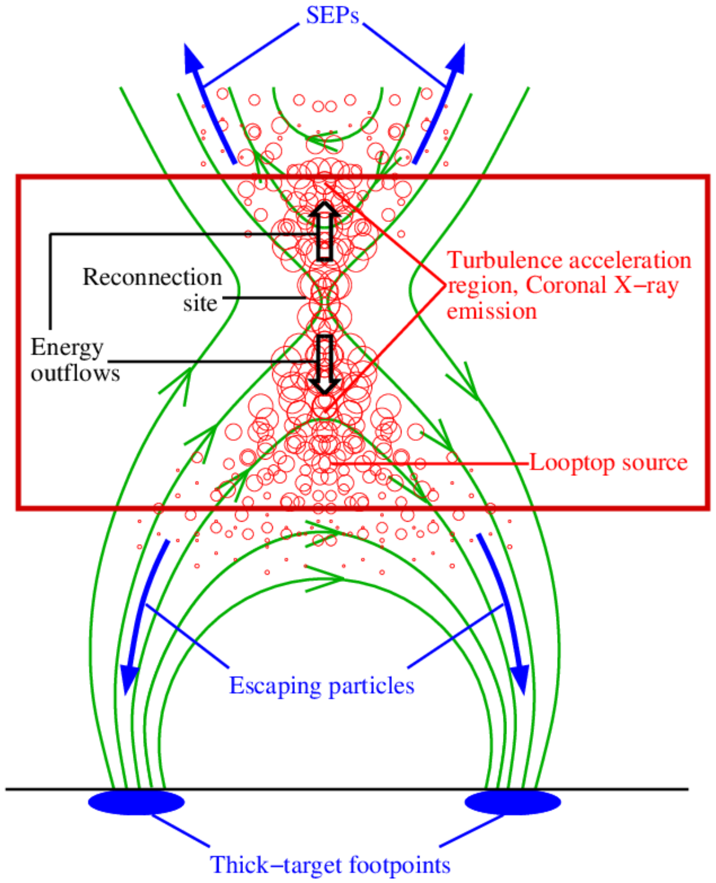

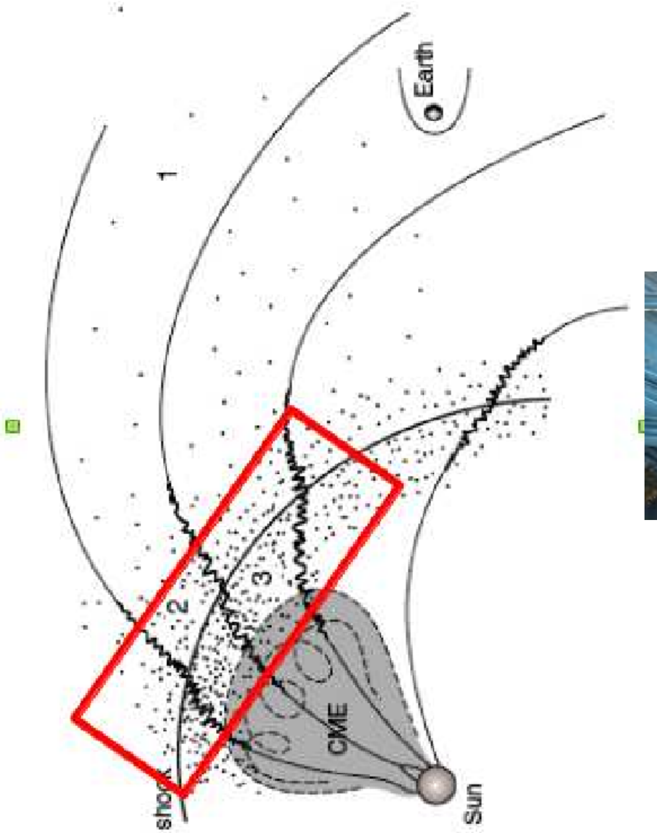

Credit: Petrosian 2016

Particle transport

Motivation

Study the acceleration of solar energetic electrons sampling events closer to the acceleration site

Study the evolution of particle parameters with distance to the Sun

To study new parameters that could be related to particle acceleration processes

Solar activity relations in energetic electron events measured by the MESSENGER mission

Rodríguez-García et al. (A&A, 2023b)

L. Rodríguez-García, L. A. Balmaceda, R. Gómez-Herrero, A. Kouloumvakos, N. Dresing, D. Lario, I. Zouganelis, A. Fedeli, F. Espinosa Lara, I. Cernuda, G. C. Ho, R. F. Wimmer–Schweingruber, and J. Rodríguez-Pacheco

Credit: https://ismaelcaracol.wordpress.com/

Pictures and screenshots are welcome

Link to the article

MESSENGER: solar energetic electrons observations

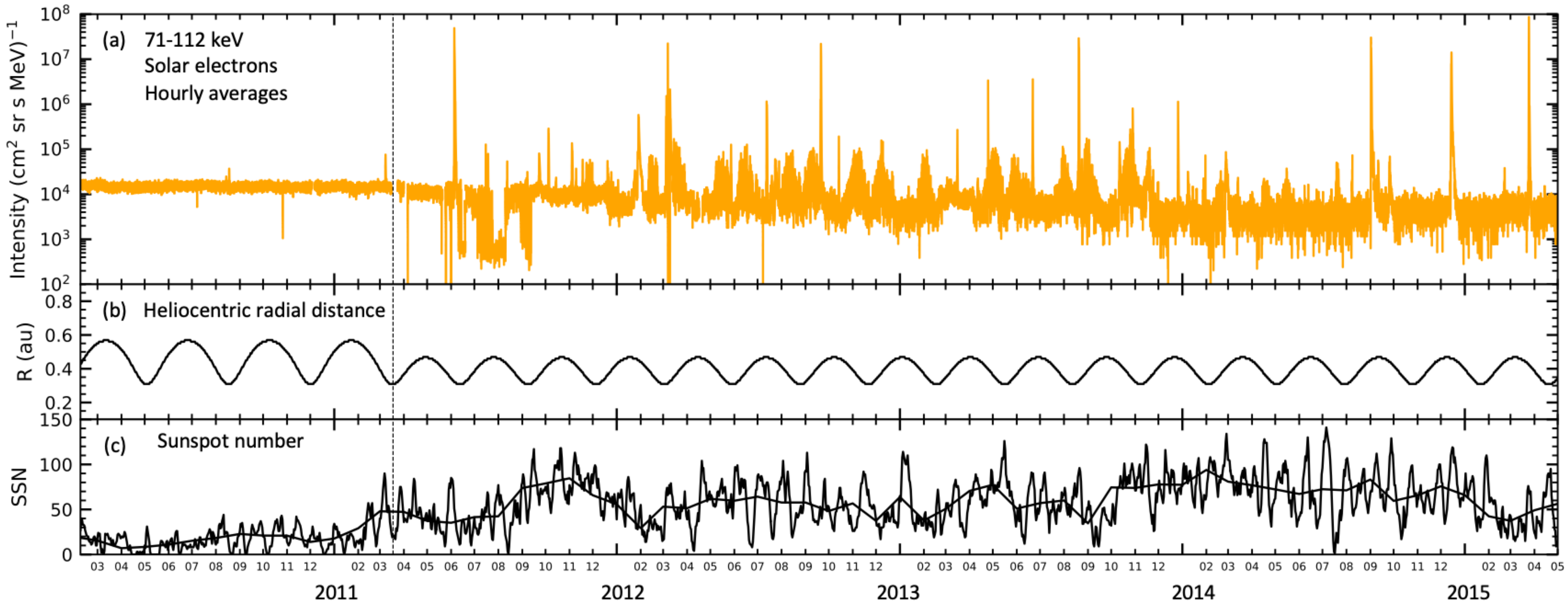

- Most of the rising, maximum, and early decay phase of solar cycle 24
- Heliocentric distance of MESSENGER: 0.31 to 0.47 au
- 61 solar energetic electron events (vertical spikes)
- High background of MESSENGER/EPS instrument-> only strong events
- Anti-Sun pointing of MESSENGER/EPS-> lower limit of peak electron intensities

In situ electron increases versus solar activity

Example: Solar energetic electron event on 2011 June 4

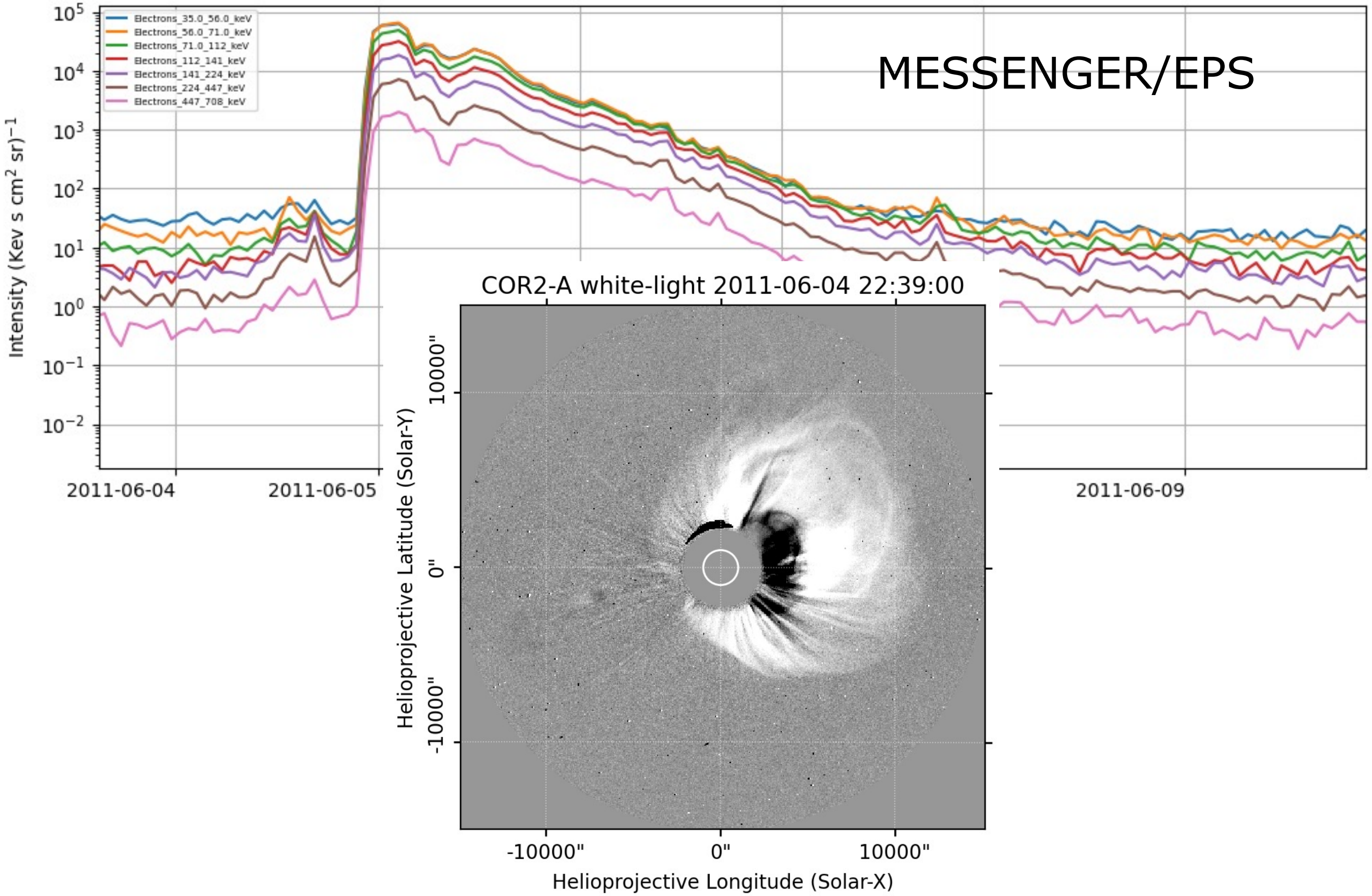

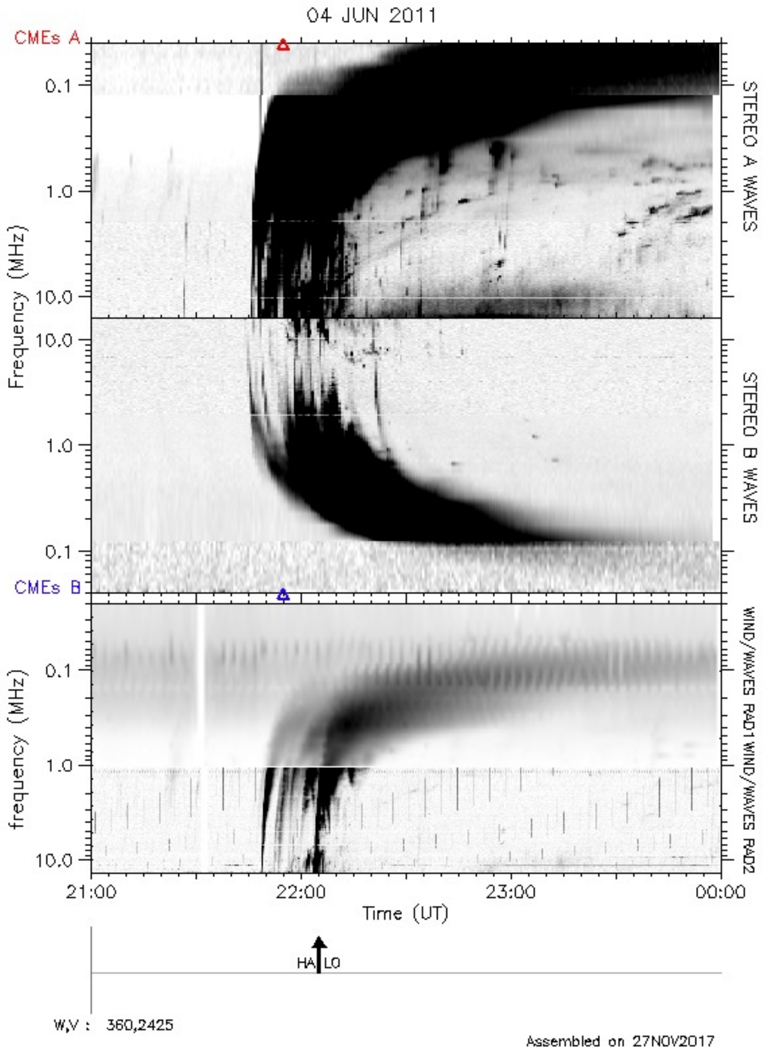

Parker spiral/3D CME & CME-driven shock

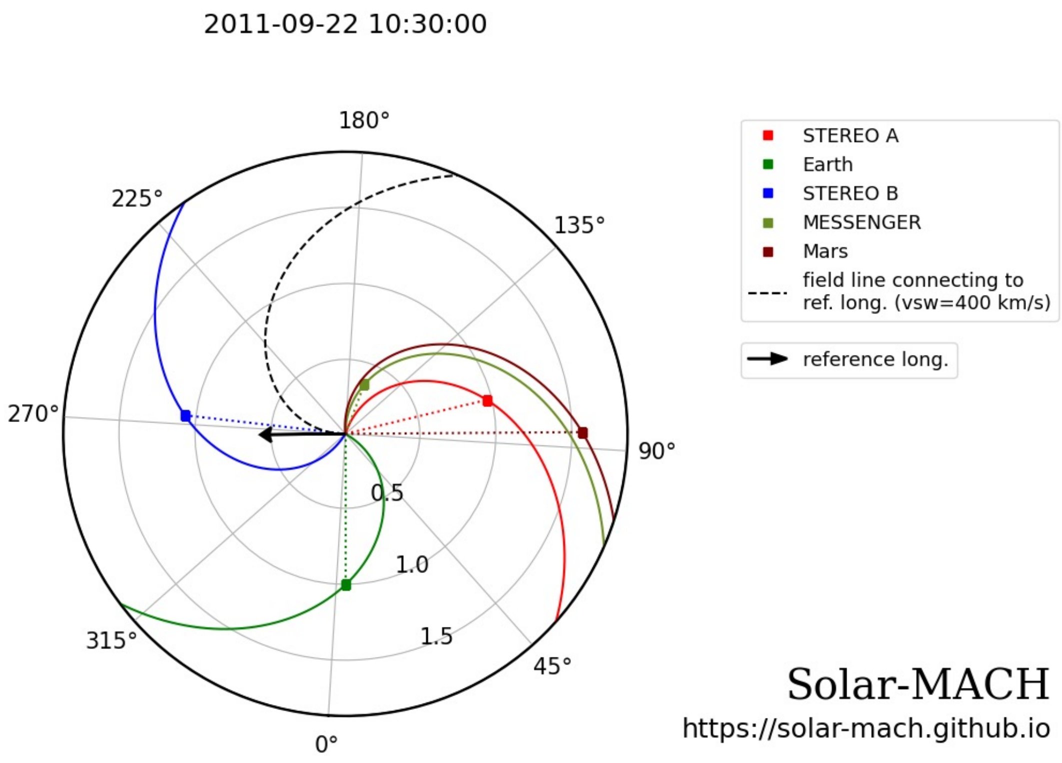

Nominal connection angle (CA) using 400 km/s solar wind speed

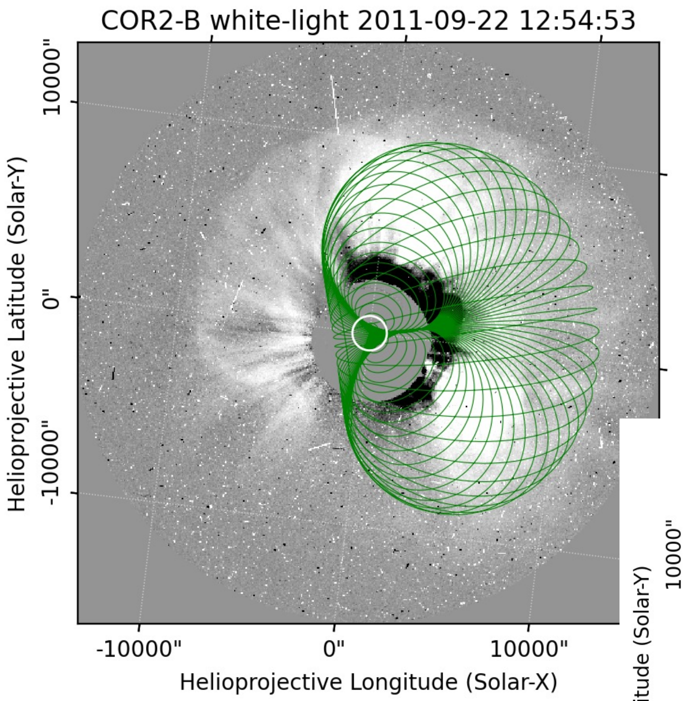

3D CME/CME-driven shock geometry and kinematics

PyThea

Reconstruct the 3D structure of CMEs and shock waves

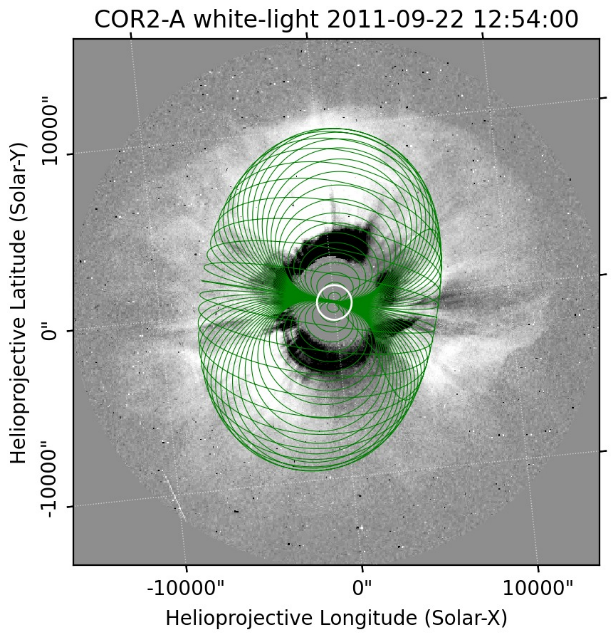

Relations: e⁻ peak intensity vs solar source parameters

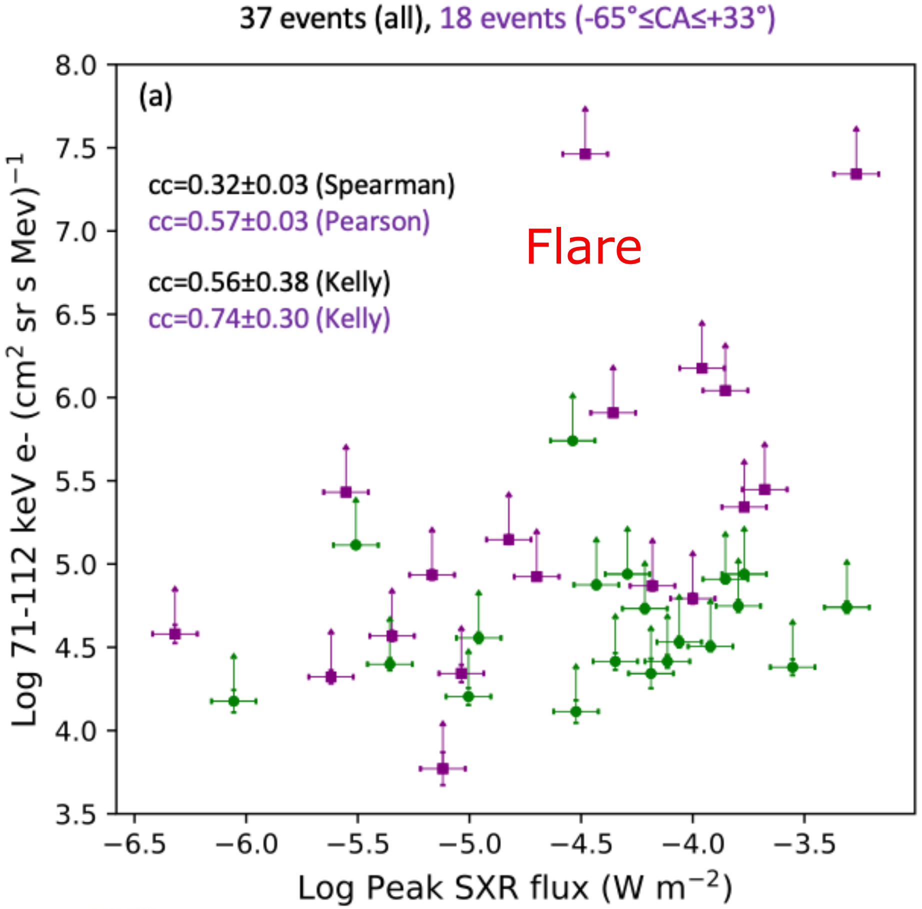

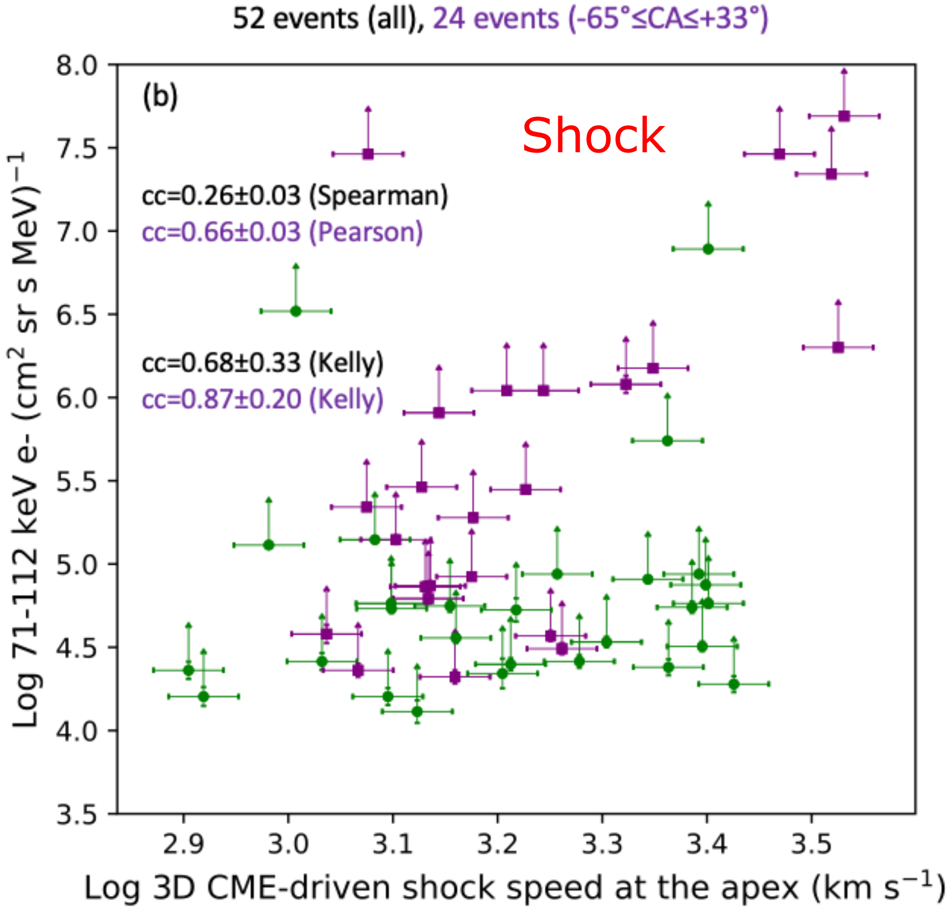

- ❑ Spearman, Pearson, and Kelly correlation methods used
- ❑ Corrected for the lower limit of peak intensity values measured by MESSENGER

Similar correlations (within uncertainties) between the SEE peak intensities and the flare or shock parameters

Relations: e⁻ peak intensity vs solar source parameters

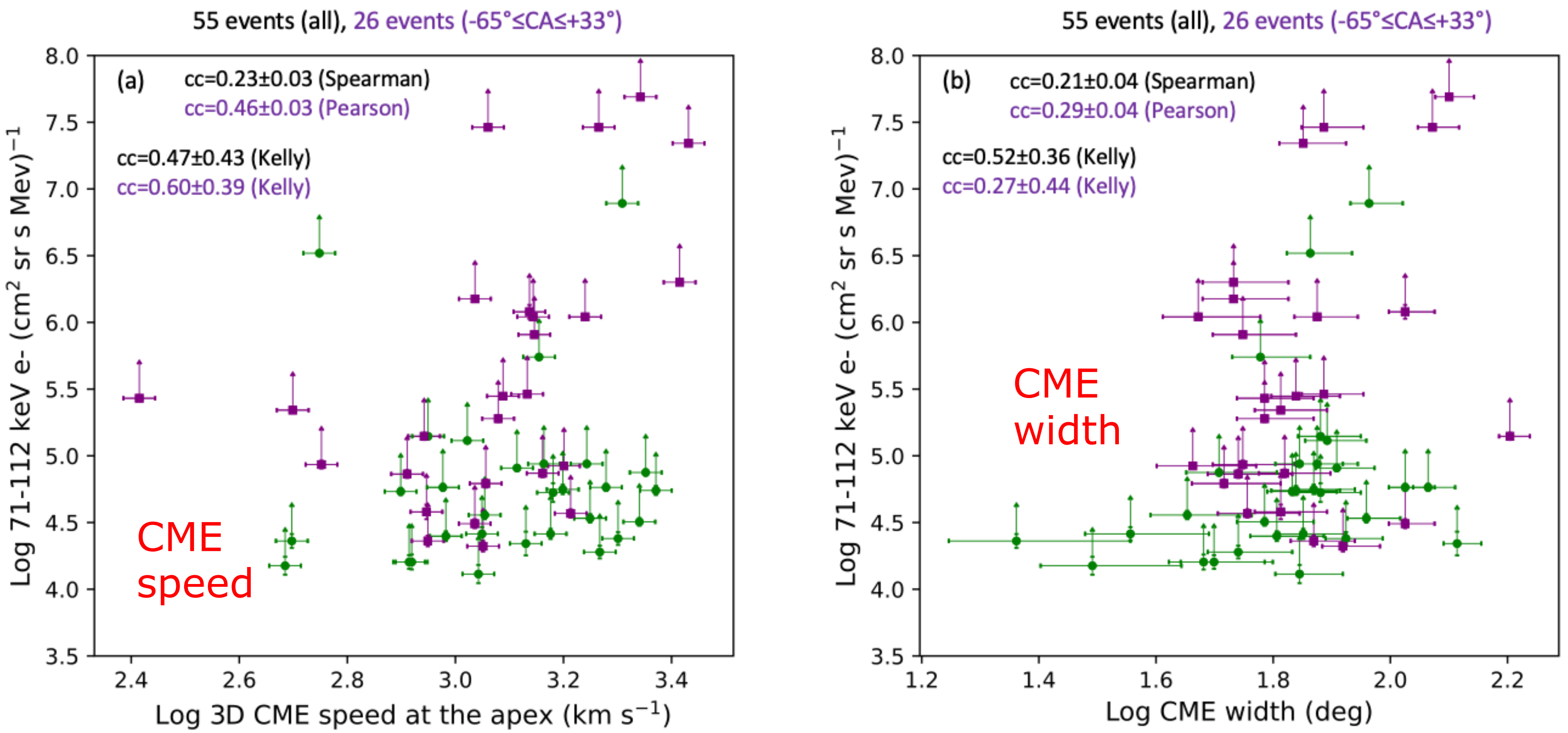

- Spearman, Pearson, and Kelly correlation methods used
- Corrected for the lower limit of peak intensity values measured by MESSENGER

The correlation of the peak electron intensity with the maximum speed of the 3D CME-driven shock at the apex is stronger than that with the 3D CME speed at the apex

The 3D CME geometry plays a moderate role in the acceleration of particles

Solar energetic electrons (SEE) measured by the MESSENGER and Solar Orbiter missions

Peak intensity and peak-intensity energy spectrum radial dependences: statistical analysis

Rodríguez-García et al. (A&A 2023a)

L. Rodríguez-García, R. Gómez-Herrero, N. Dresing, D. Lario, I. Zouganelis, L. A. Balmaceda, A. Kouloumvakos, A. Fedeli, F. Espinosa Lara, I. Cernuda, G. C. Ho, R. F. Wimmer–Schweingruber, and J. Rodríguez-Pacheco

Credit: https://ismaelcaracol.wordpress.com/

Pictures and screenshots are welcome

Link to the article

Nominal Parker spiral alignment with near 1 au

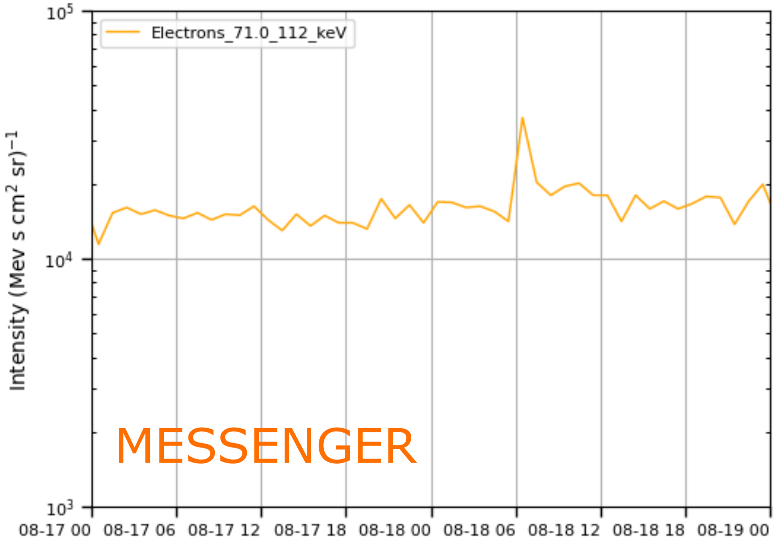

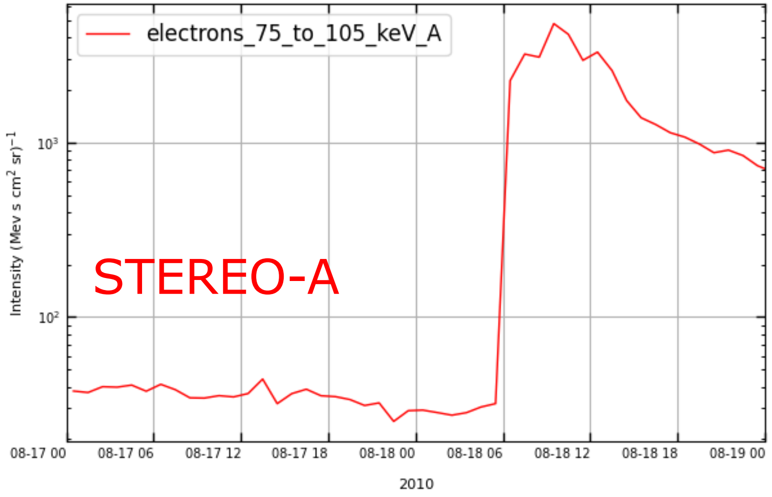

We have corrected for:

1. Small longitudinal effect (not exactly the same connectivity to the source)
2. Intercalibration factor between s/c to compare the peak intensities

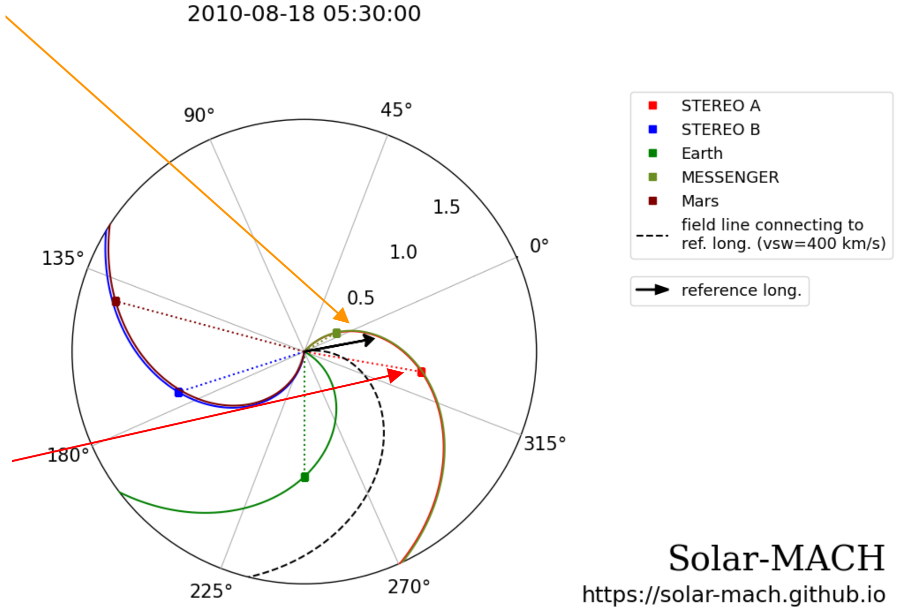

Similar connectivity is not always guaranteed

Large sample of events is instrumental to derive radial dependences

Radial dependence of the e⁻ peak intensities

esa

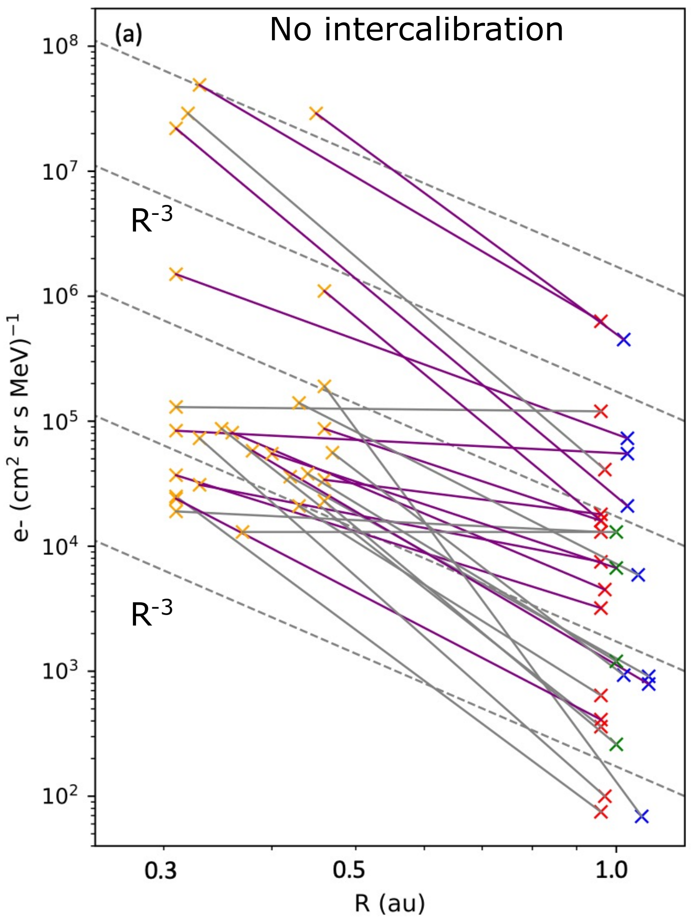

$\sim R^{\alpha}$

SEP 1: α =-5.14	+0.41
SEP 2: α =-2.17	-0.03
SEP 4: α =-1.33	-0.09
SEP 5: α =-4.08	-0.06
SEP 8: α =-2.92	+0.35
SEP 12: α =-3.86	-2.35
SEP 13: α =-4.08	+0.22
SEP 14: α =-4.35	+1.21
SEP 15: α =-0.86	-0.16
SEP 16: α =-2.30	-0.51
SEP 17: α =-0.35	-0.03
SEP 18: α =-2.52	+0.02
SEP 19: α =-5.79	+0.87
SEP 21: α =-5.44	+0.47
SEP 22: α =-0.34	-0.52
SEP 23: α = -0.07	+0.30
SEP 30: α =-9.38	+0.75
SEP 34: α =-3.60	+0.34
SEP 37: α =-5.92	+0.67
SEP 38: α =-3.51	-1.15
SEP 45: α =-5.75	+0.30
SEP 50: α =0.00	-1.62
SEP 51: α =-2.30	+0.08
SEP 52: α =-5.77	+0.92
SEP 53: α =-6.11	+0.67
SEP 54: α =-5.09	-0.72
SEP 57: α =-5.29	+1.11
SEP 60: α =-4.21	+0.99

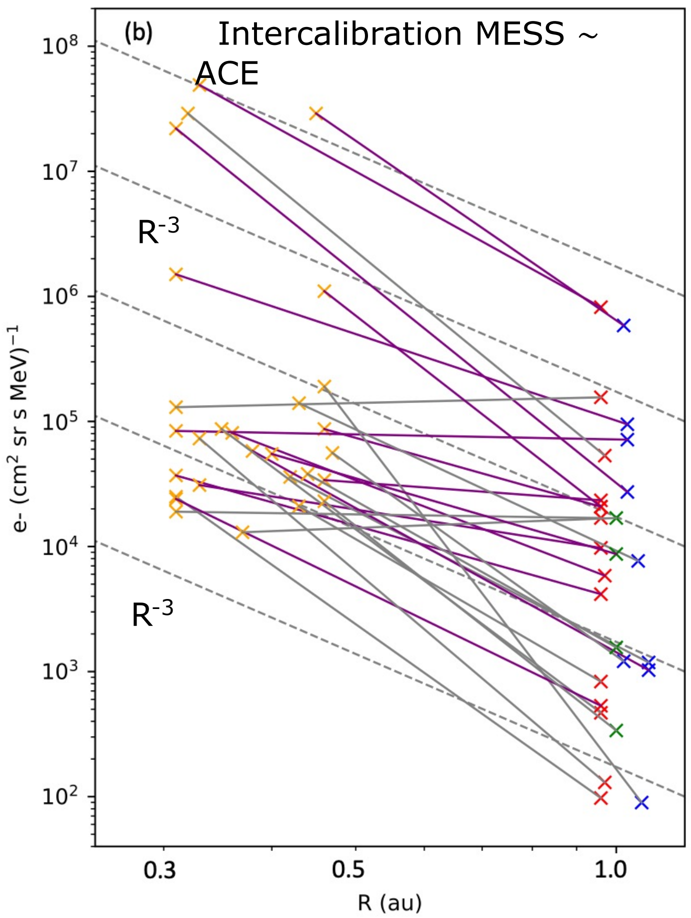

$\sim R^{\alpha}$

SEP 1: α =-4.91	+0.41
SEP 2: α =-1.93	-0.03
SEP 4: α =-1.08	-0.09
SEP 5: α =-3.83	-0.06
SEP 8: α =-2.65	+0.35
SEP 12: α =-3.58	-2.35
SEP 13: α =-3.83	+0.22
SEP 14: α =-4.02	+1.21
SEP 15: α =-0.51	-0.16
SEP 16: α =-1.94	-0.51
SEP 17: α =-0.13	-0.03
SEP 18: α =-2.30	+0.02
SEP 19: α =-5.57	+0.87
SEP 21: α =-5.18	+0.47
SEP 22: α =-0.10	-0.52
SEP 23: α =0.16	+0.30
SEP 30: α =-9.07	+0.75
SEP 34: α =-3.37	+0.34
SEP 37: α =-5.68	+0.67
SEP 38: α =-3.22	-1.15
SEP 45: α =-5.39	+0.30
SEP 50: α =0.26	-1.62
SEP 51: α =-2.01	+0.08
SEP 52: α =-5.43	+0.92
SEP 53: α =-5.87	+0.67
SEP 54: α =-4.77	-0.72
SEP 57: α =-4.95	+1.11
SEP 60: α =-3.89	+0.99

SEE events where CA difference < |20|º

SEE events where CA difference < |30|º

MESSENGER: 71-112 keV

STEREO-A: 75-105 keV
STEREO-B: 75-105 keV
ACE: 53-103 keV

Radial dependence of the e^- peak intensities

(a) No longitudal effect correction
No intercalibration

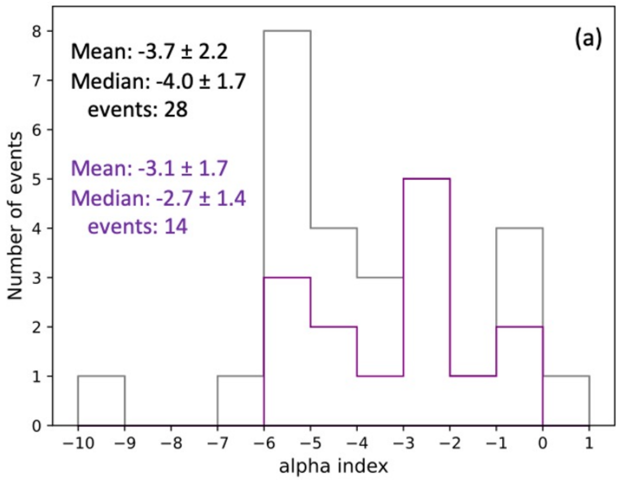

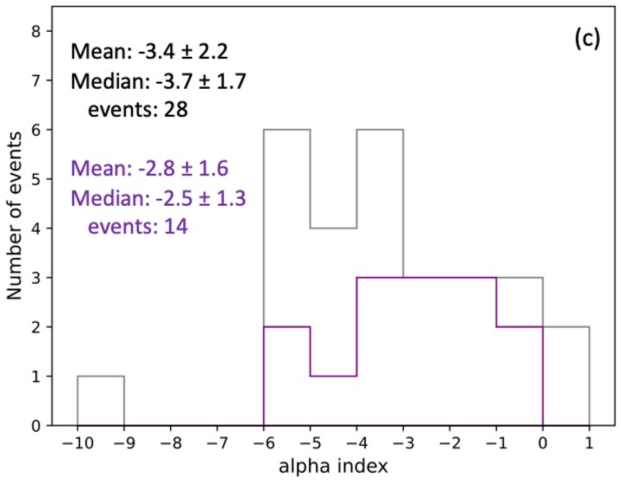

(c) No longitudinal effect correction
Intercalibration

(b) Longitudal effect correction
No intercalibration

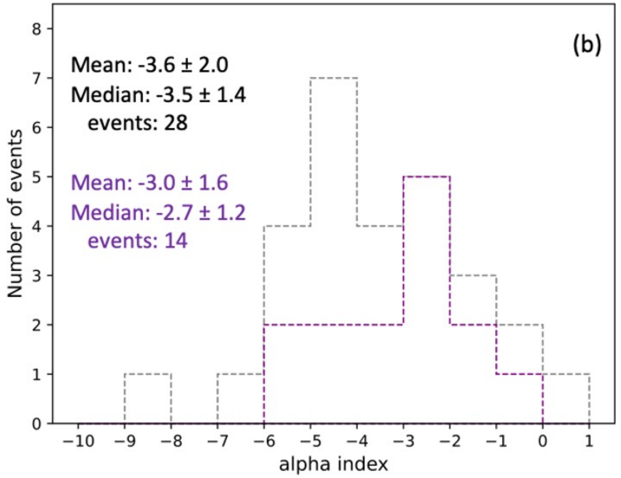

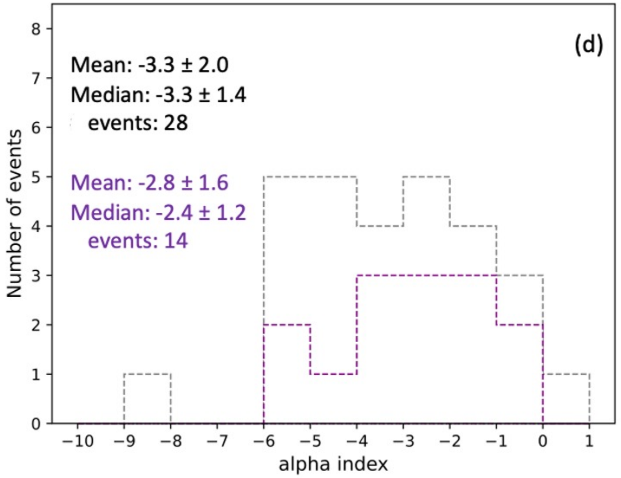

(c) Longitudal effect correction & Intercalibration

On average and within the uncertainties, the **dependence R^{-3}** found in previous studies **is confirmed**

e^- peak-intensity energy spectrum near 0.4 au

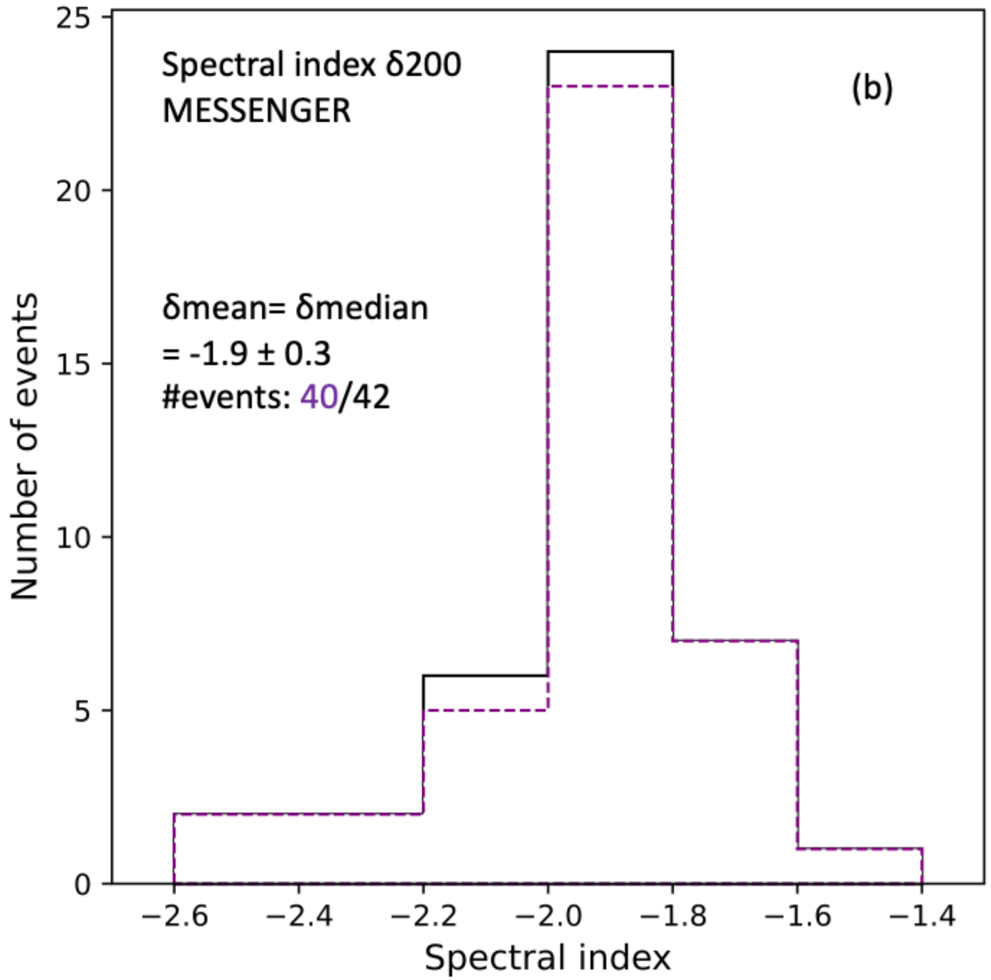

Spectral indices	Near 0.4 au (this study) Backward spectra	Near 1 au Forward spectra
δ200	-1.9 ± 0.3 	-3.55 ± 1.45 (Dresing et al., 2020)
		-2.56 (Dresing et al., 2022)

Radial dependence of the e⁻ energy spectrum

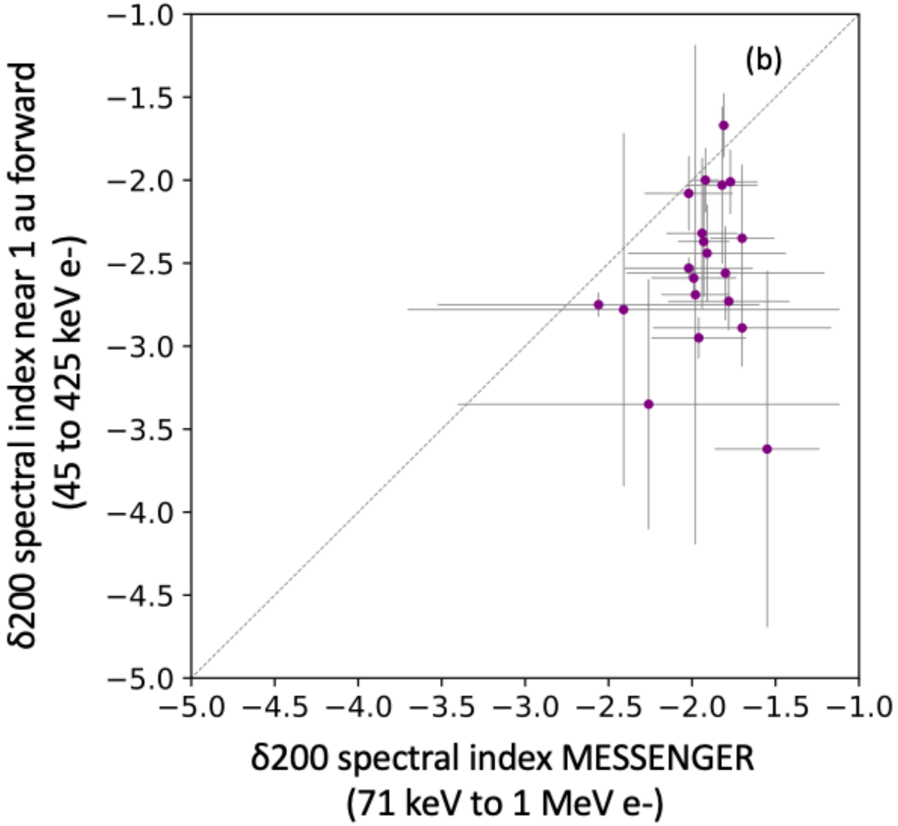

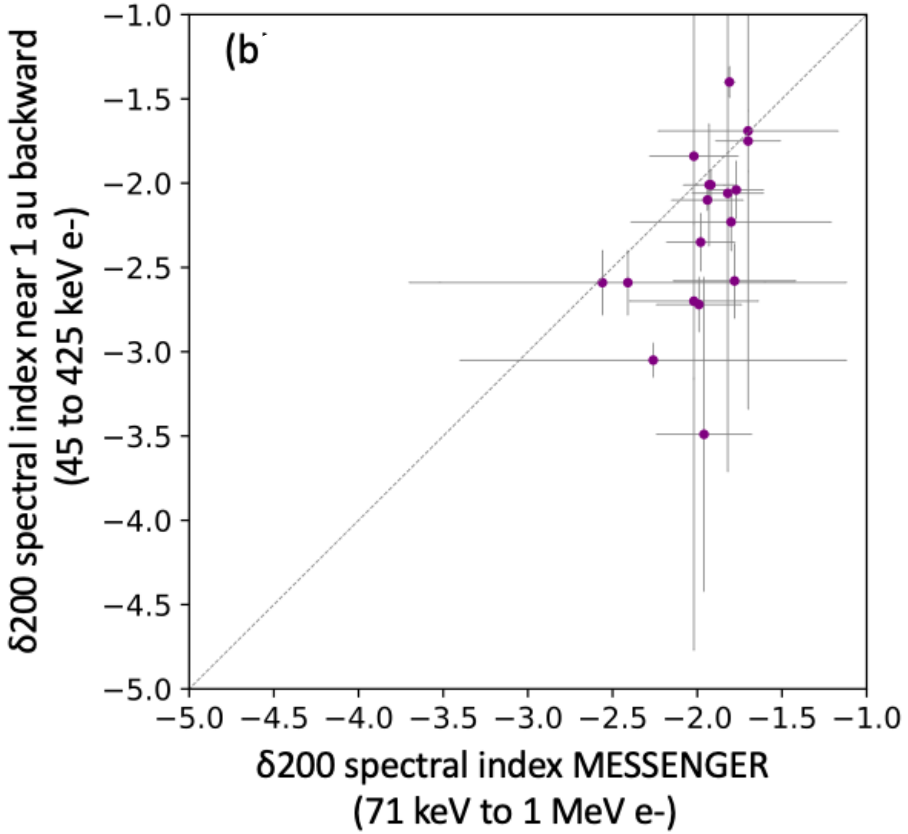

The **electron spectral index** found in the energy range around 200 keV (δ200) of the backward-scattered population **near 0.3 au is harder when compared to** the both anti-sunward and backward propagating beam **near 1 au.**

What CME properties account for SEP events?

Balmaceda et al. (ApJ, in prep.)
L. A. Balmaceda, L. Rodríguez-García, Angelos Vourlidas,
David Lario, Raúl Gómez-Herrero, and Nina Dresing

Particles near 1 au (prompt component of the peak intensities from STEREO-A, STEREO-B, ACE, and SOHO)

- **Electrons**: near-relativistic (70-100 keV) and relativistic (1 MeV)
- **Protons**: 5 MeV, 25 MeV, 50 MeV

Possible accelerators:

- Flare peak, fluence
- CME 3D kinematics
- Wave 3D kinematics

Example of remote-sensing coverage

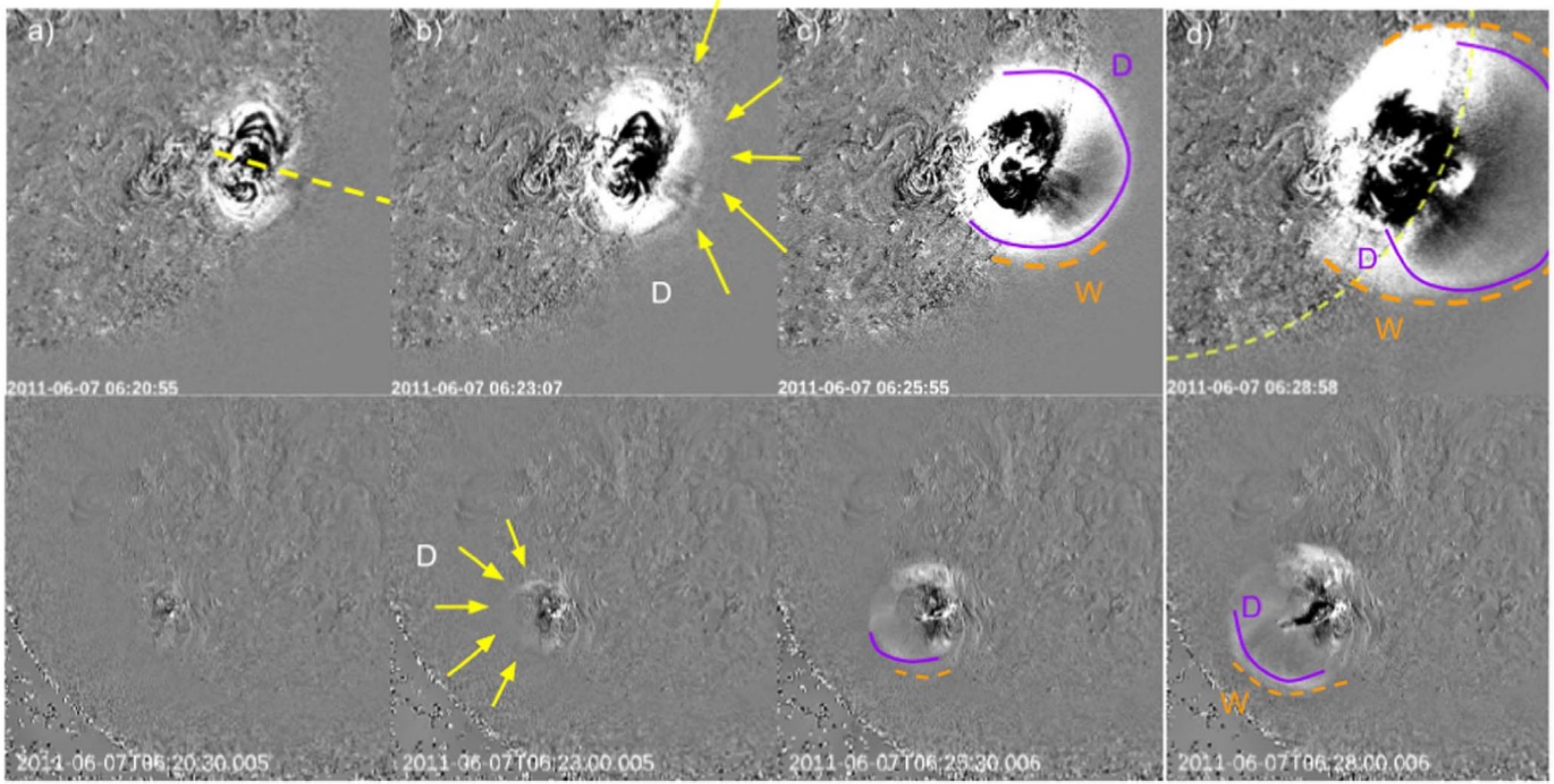

Figure 5. 2011 June 7 event as seen by AIA (top) and EUVI-A (bottom). The sequence shows different stages in the CME early evolution and wave formation. (a) Rising filament. (b) Early CME (bubble) formation. (c) Lateral expansion of the CME, D, leading to the formation of the wave, W. (d) The separation of the wave (W; orange line) from the driver (D; purple line) is clearly observed. All frames are base-difference images. The yellow dashed lines in panels (a) and (d) indicate the direction for the radial and circular slits used to build the stackplots in Figure 6. An animation of the bottom panels of this figure is available. The animation includes the EUVI-A 195 Å image on the left and the corresponding base-difference image on the right. The animation sequence starts at 06:00:30 UT and ends at 06:38:00 UT. The time lapse between images is 2.5 minutes.

Balmaceda et al, 2022 ApJ

Link to the article

Parameters of CME & wave included in the study

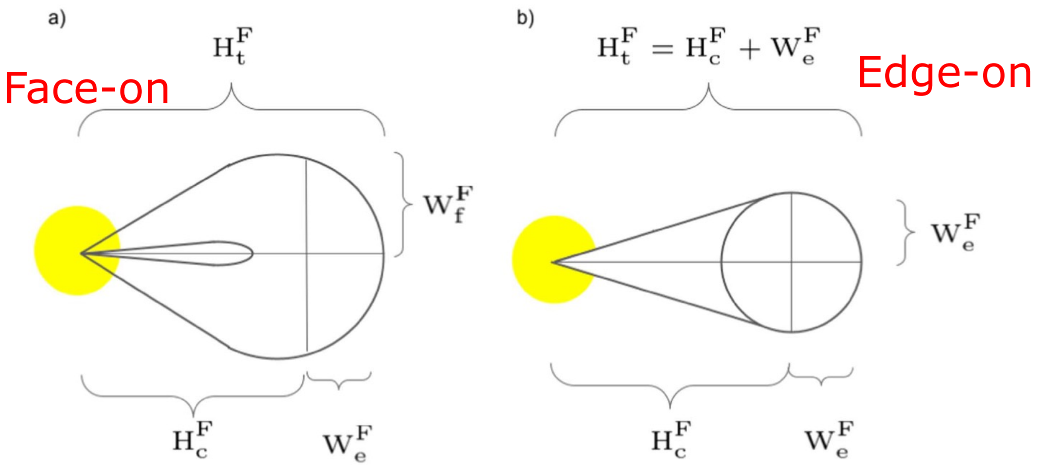

Balmaceda et al, 2022 ApJ

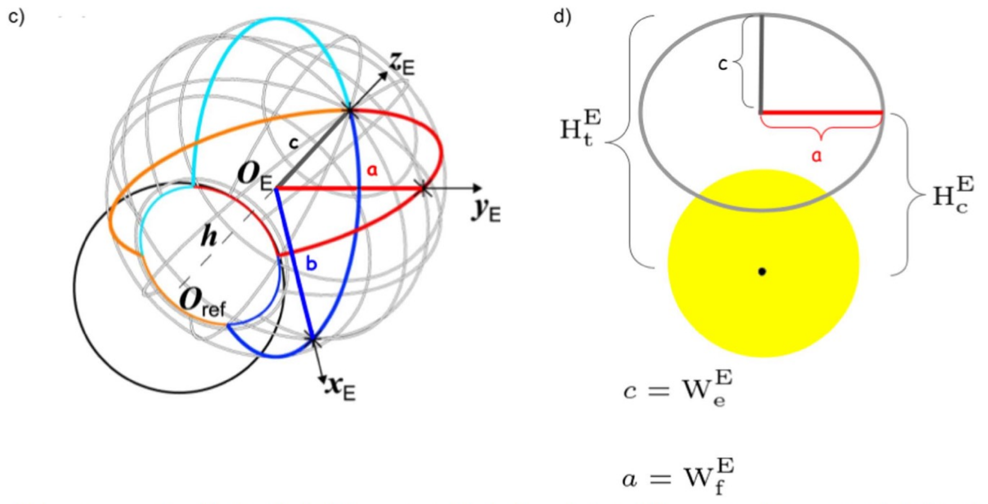

Figure 1. Schematic representation of the 3D models for the flux rope (top) and the shock/wave (bottom) with the parameters of interest (see text for details). (a) Face-on view of the flux rope. (b) Edge-on view of the flux rope. (c) Ellipsoid model (adapted from Kwon et al. 2014). (d) Simplified 2D version of the shock/wave model.

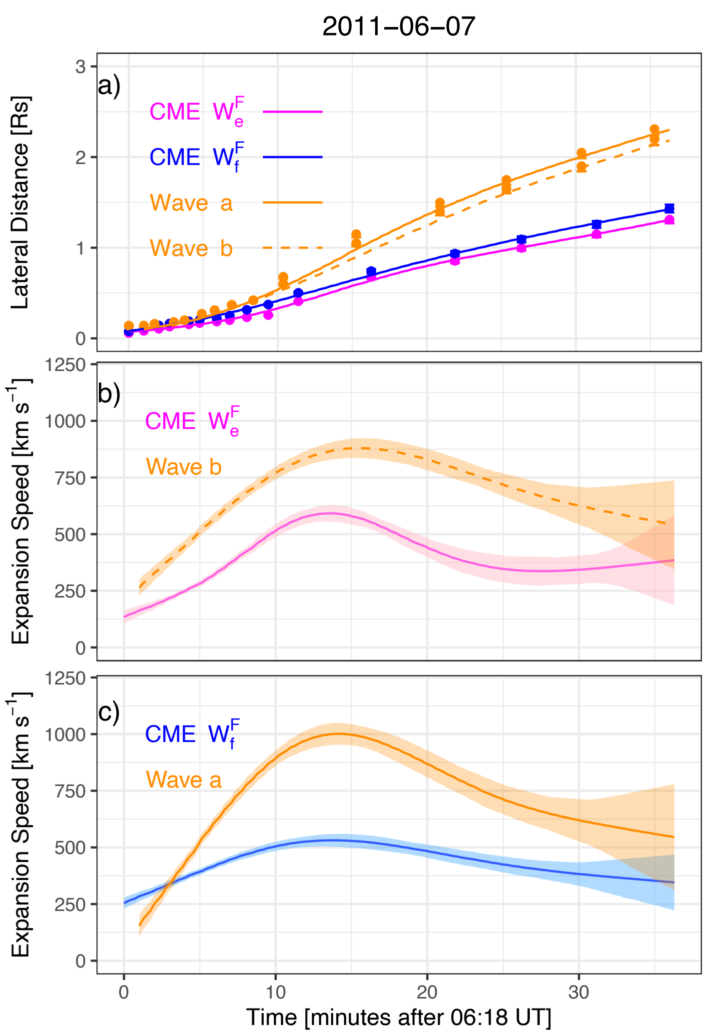

Preliminary list of events under study

Event	Date	Location	CME v_{peak} [km s^{-1}]			Shock v_{peak} [km s^{-1}]	
		Lat,Long	LE	WEO	WFO	Top	b
1	12/12/2013	S29W45	1257	503	626	1279	734
2	11/19/2013	S15W75	1250	255	500	1350	875
3	06/21/2013	S20E72	2000	750	1100	2000	900
4	05/22/2013	N17W76	1757	721	1161	1951	1339
6	05/26/2012	N17W120	2385	642	1000	2621	1481
7	05/17/2012	N06W81	2583	1105	1578	2664	2117
8	10/20/2011	N17W100	1009	343	424	1022	586
10	09/22/2011	N20E70	1832	593	827	1851	886
11	08/09/2011	N21W70	1878	717	932	1937	1286
12	08/08/2011	N18W62	2065	633	822	2095	1088
13	08/04/2011	N24W36	2385	637	903	2405	1291
14	03/07/2011	N10E20	960	272	355	974	553
15	02/24/2011	N13E82	2019	314	826	2052	905
16	01/28/2011	N18W88	725	280	379	1092	756
17	12/31/2010	N14W55	459	462	457	531	548
18	09/08/2010	N24W93	949	319	435	966	562
19	08/18/2010	N12W100	1670	379	839	1669	883
20	08/14/2010	N10W53	1275	277	457	1287	798

CME:
-LE (leading edge): radial expansion

-WEO (width edge-on): cross-section expansion

-WFO (width face-on): lateral expansion

CME-driven shock:
-Top: radial expansion

-b: lateral expansion

Example of spacecraft constellation

SEP event number 1

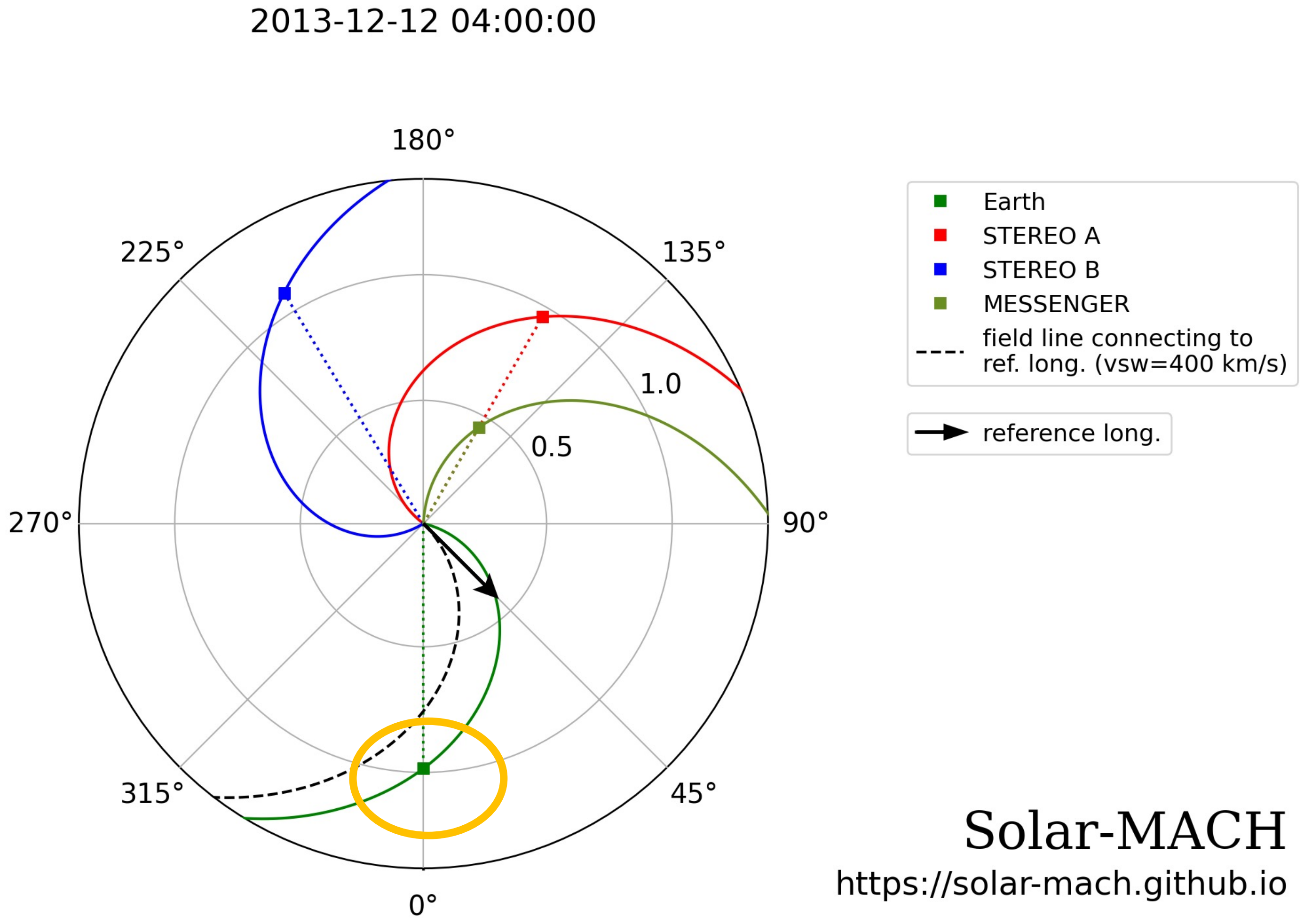

Solar-MACH

https://solar-mach.github.io

Near-relativistic electrons (70-100 keV)

esa

CME

radial

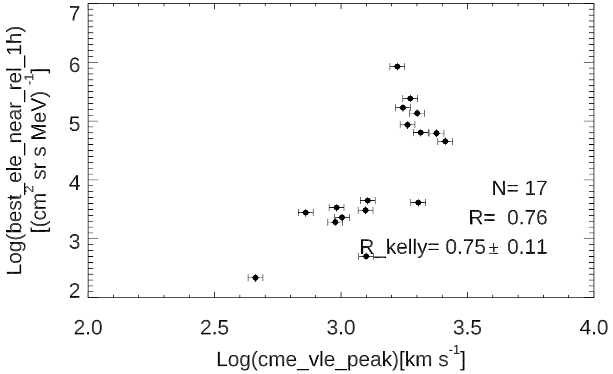

lateral

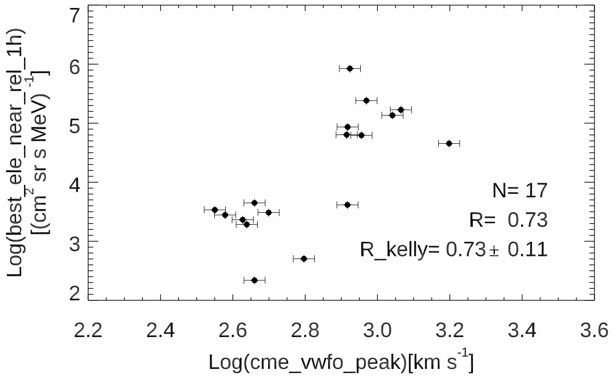

cross-section

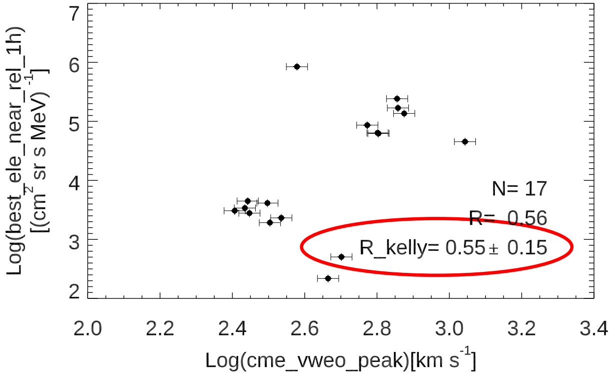

Wave

radial

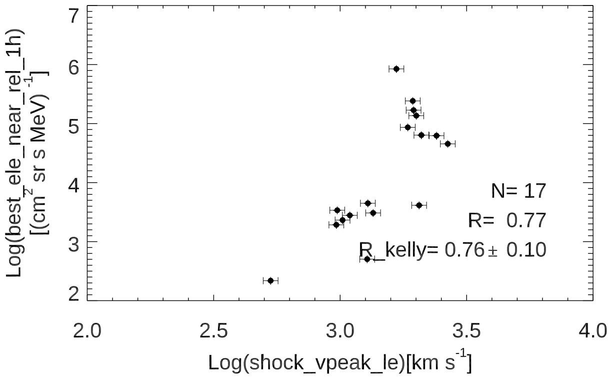

lateral

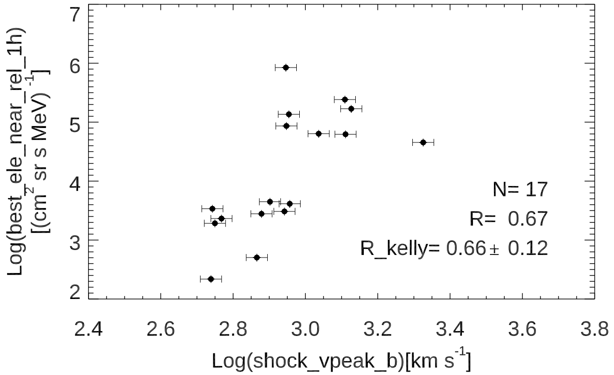

Best connected s/c

Lateral expansion of the CME **more relevant** than the cross-section expansion

Relativistic electrons (1 MeV)

CME

radial

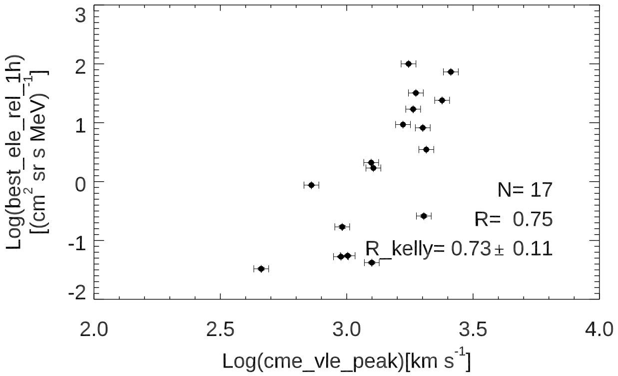

lateral

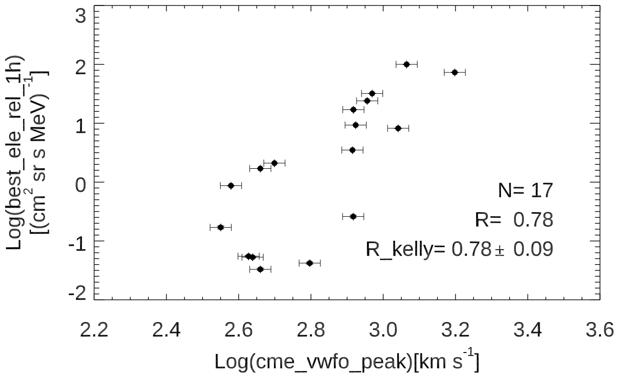

cross-section

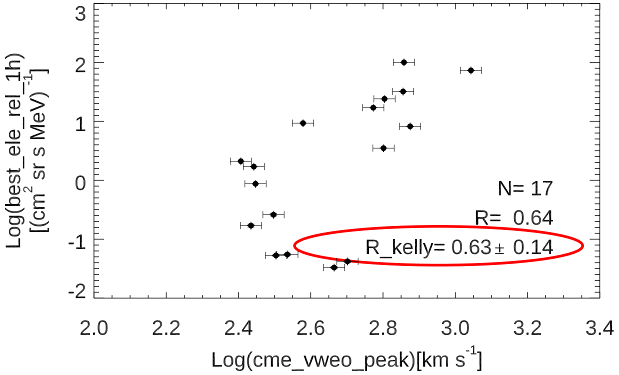

Wave

radial

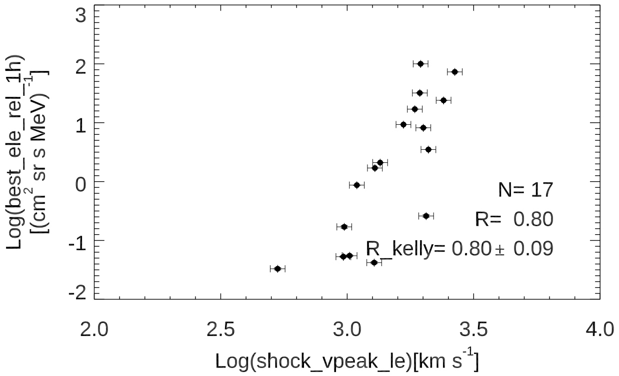

lateral

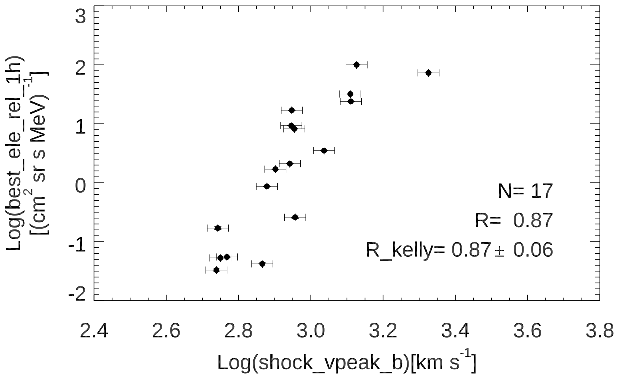

Best connected s/c

Lateral expansion of the CME **more relevant** than the cross-section expansion

5 MeV protons

CME

radial

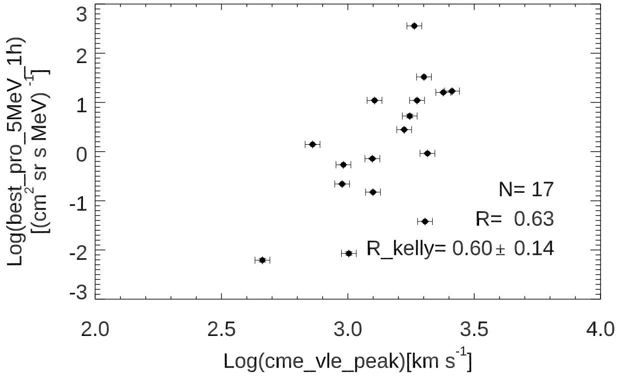

lateral

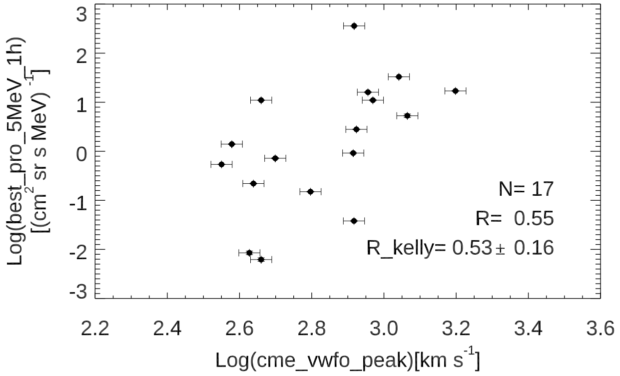

cross-section

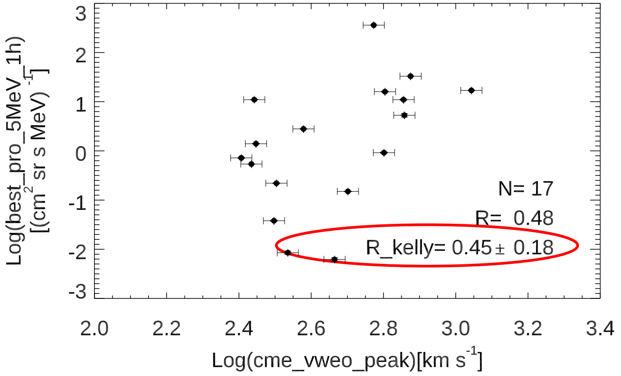

Wave

radial

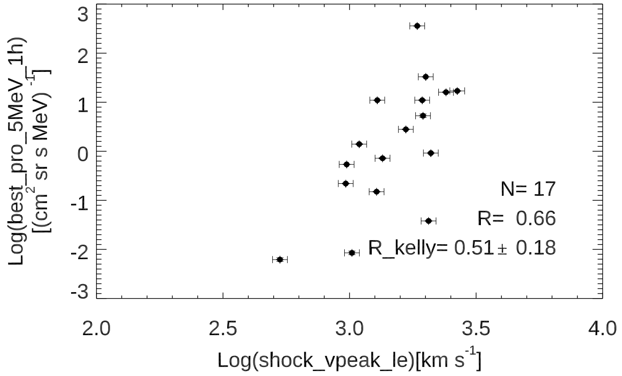

lateral

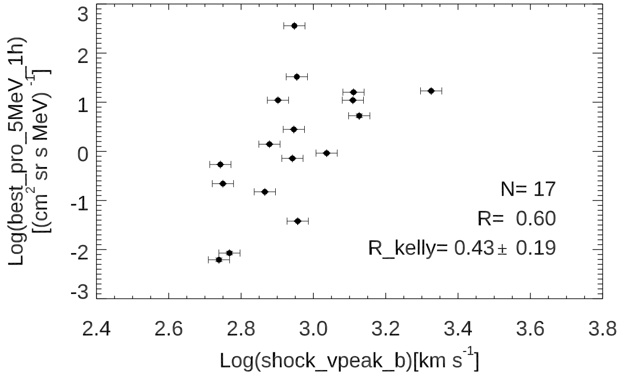

Best connected s/c

Lateral expansion of the CME **more relevant** than the cross-section expansion

25 MeV protons

CME

radial

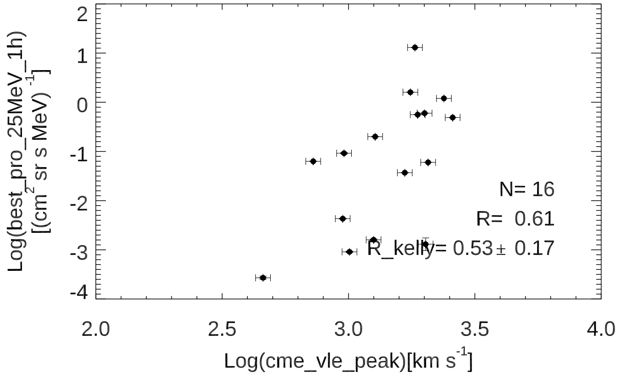

Wave

radial

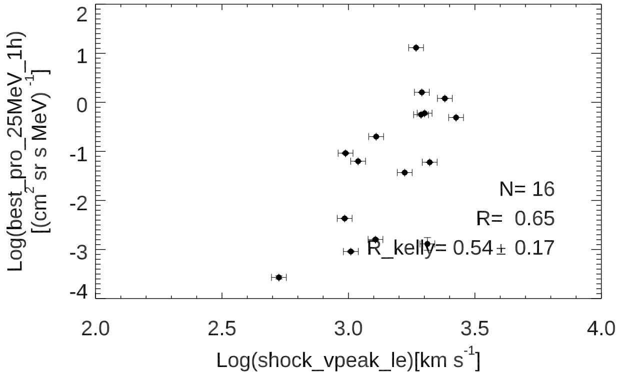

lateral

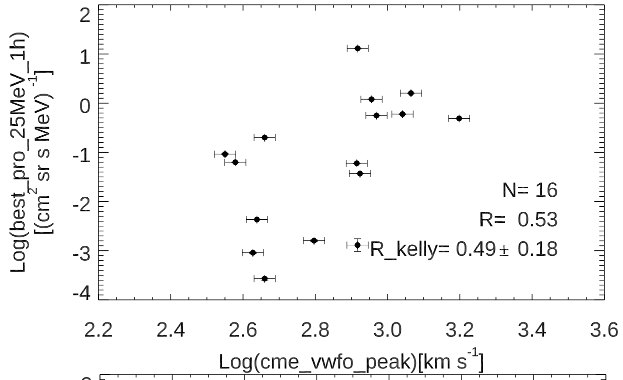

lateral

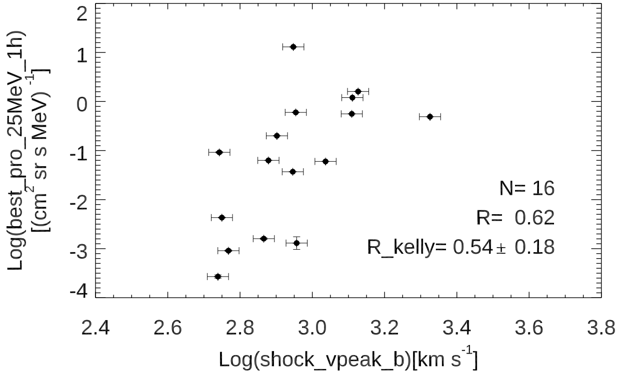

Best connected s/c

cross-section

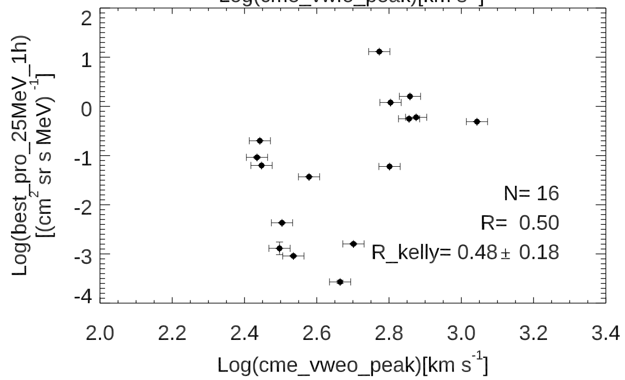

Shock speed and CME speed have **similar relevance**

50 MeV protons

CME

radial

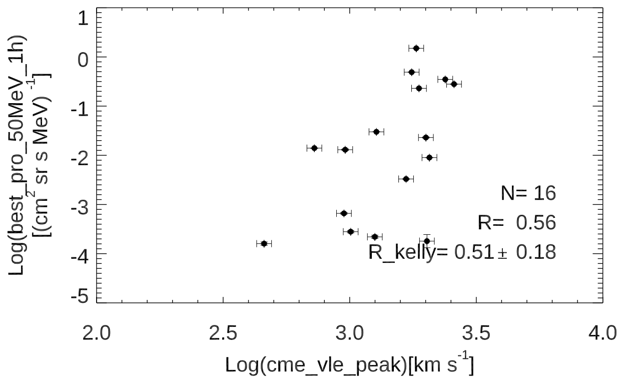

lateral

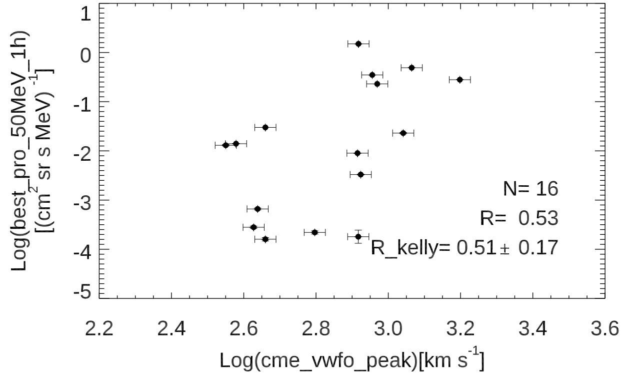

cross-section

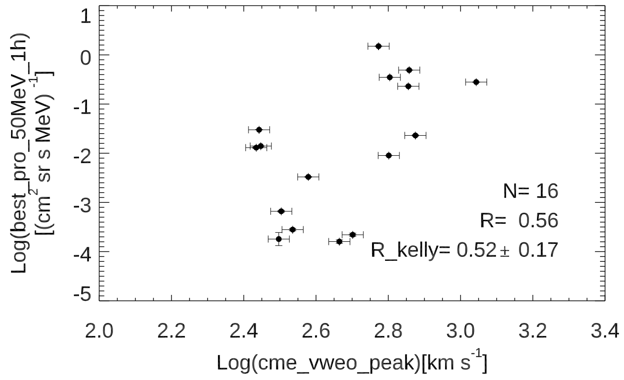

Wave

radial

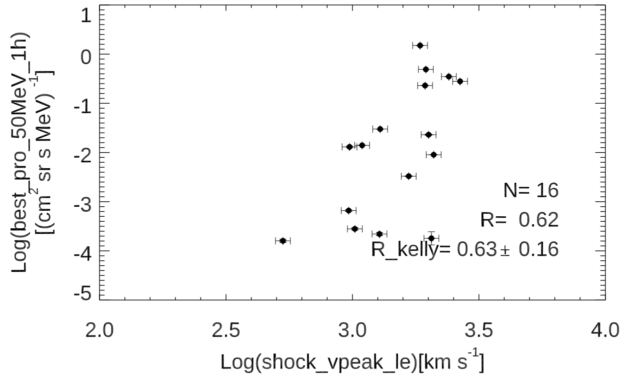

lateral

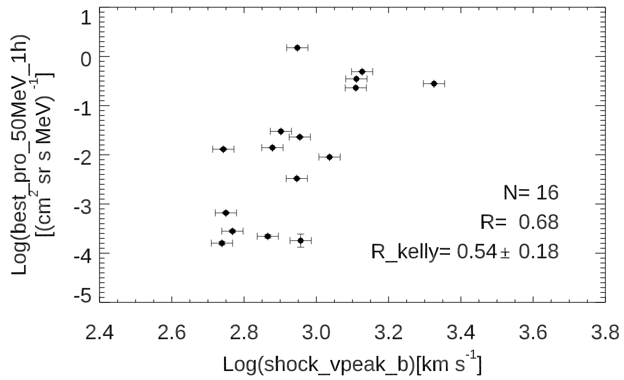

Best connected s/c

Shock speed and CME speed have **similar relevance**

Conclusions

esa

- ✓ **Both flare and shock-related processes may contribute to the acceleration of near relativistic electrons in large SEE events,** in agreement with previous studies based on near 1 au data

- ✓ **The maximum speed of the CME-driven shock is a better parameter to investigate particle-acceleration-related mechanisms than the average CME speed,** as suggested by the stronger correlation with the SEE peak intensities

- ✓ There is a wide variability in the radial dependence of the electron peak intensity between ~0.3 au and ~1 au, but the peak intensities of the energetic electrons decrease with radial distance from the Sun in 27 out of 28 events. **On average and within the uncertainties, we find a radial dependence consistent with R^{-3}**

- ✓ The **electron spectral index** found in the energy range around 200 keV (δ200) of the backward-scattered population **near 0.3 au is harder** in 19 out of 20 (15 out of 18) events by a median factor of ~20% (~10%) **when compared to** the anti-sunward propagating beam (backward-scattered population) **near 1 au.**

Conclusions

Electrons and protons 5 MeV:

- Lateral expansion of the CME **more relevant** than the cross-section expansion

Protons 25 and 50 MeV:

- Shock speed and CME speed have **similar relevance**
- **Similar relevance** of CME and shock-lateral, cross-section- expansion speeds

Acceleration and Transport of Solar Energetic Particles in the Inner Heliosphere

laura.rodriguezgarcia@esa.int